1990

Scroll Compressor Flow Modeling: Experimental and Computational Investigation

R. J. Rogers
United Technologies Research Center

R. C. Wagner
United Technologies Research Center

SCROLL COMPRESSOR FLOW MODELING: EXPERIMENTAL AND COMPUTATIONAL INVESTIGATION

Richard J. Rodgers
Research Engineer
Phone: 203/727-7224

Timothy C. Wagner
Associate Research Engineer
Phone: 203/727-7371

United Technologies Research Center
East Hartford, CT 06108

ABSTRACT

An experimental and computational investigation of the flow field in the final compression and discharge region of a scroll compressor was conducted to obtain a detailed understanding of the fluid dynamic loss mechanisms. The experimental investigation utilized flow visualization techniques and pressure loss measurements to characterize the flow. The computational investigation involved three-dimensional finite element modeling of the experimental flow. Typical flow patterns are presented and compared with calculated flow velocity vectors.

INTRODUCTION

Scroll vapor compressors are being recognized by the HVAC industry as being highly competitive with conventional compressors. Scroll units offer potential cost, operational, and environmental advantages expressed in terms of their high efficiency, reduced part requirements, lower noise, and reduced vibration levels. Further increases in efficiency may be realized if the flow losses, particularly in the final compression and discharge region, were reduced. (According to Ref. 1, approximately 3 percent of the input power is consumed due to flow losses.) An understanding of the flow processes occurring in the discharge region is necessary to devise a means of reducing these flow losses, which become more pronounced with operation at increased speed. This paper presents one method of studying the complex flow patterns that exist in the discharge region.

A flow visualization experiment and a companion Computational Fluid Dynamic (CFD) analysis were conducted of the flow in the final compression and discharge region of a scroll compressor model (see Fig. 1). Both the experiment and the analysis were performed with stationary scrolls positioned at selected crank angles. The justification for this quasi-steady approach is that the wall velocity is small compared to the flow velocities. In a scroll compressor of 3 ton size, the velocity of the orbiting scroll is approximately 10 percent of the average velocity of the discharge flow. Since neither the flow visualization experiment nor the CFD analysis showed any boundary layer effects, treatment of the flow field with stationary walls appears justified.

FACILITY DESCRIPTION

The Flow Visualization Facility, pictured in Fig. 2, consists of a scroll model, a supply system capable of delivering water or air, a discharge pipe, a system for dye injection and illumination, a video recording system (not shown), and manometers for measuring pressure. The scroll model used in this investigation (Fig. 3) is a five-times-size lucite model of the final compression pockets of a generic scroll compressor. The flow is viewed through the bottom surface of the model as seen in Fig. 3. The model is stationary but may be positioned to simulate crank angles from 45 to 180 deg. after the onset of discharge. Flow is injected at two locations from identical rectangular injection ports, each of which is the height of the flow volume. The injectors are embedded in the outer peripheral wall in the rear half of each pocket. The discharge port is located in the top surface of the model, which is in the far field of Fig. 3. The flow visualization tests were conducted using a dye injection trace flow technique with water as the working fluid. Fluorescene dye was injected

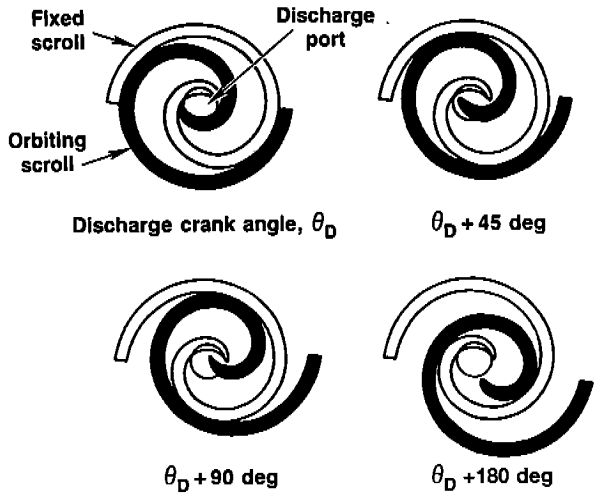

Fig. 1 Schematic of Scroll Compressor Discharge Region.

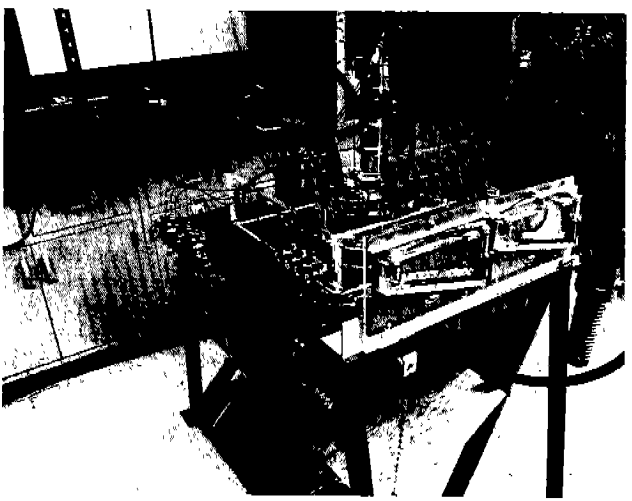

Fig. 2 Photograph of Flow Visualization Facility.

through any of three probes located in each compression pocket and was illuminated by light from an argon-ion laser. The laser beam was defocused into a sheet of light which was positioned to illuminate one of three horizontal planes: 11 percent, 50 percent (midplane), or 89 percent of the

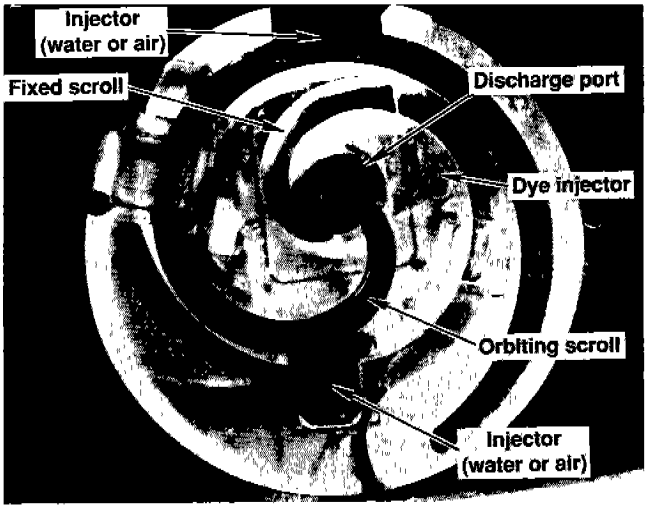

Fig. 3 Photograph of Scroll Compressor Discharge Region Model.

height of the flow volume. These axial positions correspond to the locations of the dye injection probes. Dye was injected in the plane illuminated by the laser light sheet. The flow visualization was monitored by a video camera and recorded on a video tape recorder. The tape was then played back and selected frames were photographed. Tests were also conducted using air as the working fluid so that the pressure losses of the discharge region could be quantified. Air was chosen for the working fluid because it eliminates the need to account for the static head of the water, thereby simplifying the measurement of pressure. Wall static pressures were measured at two locations on the top surface of each pocket and in the discharge pipe using slant-tube manometers.

EXPERIMENTAL RESULTS

Water flow visualization tests

For the flow visualization tests, the characteristics of the flow field were documented in the three horizontal planes previously noted for crank angles of 45, 90 and 180 deg. after onset of discharge (see Fig. 1). The water flowrate through the model was evenly distributed between the two compression pockets. The nominal Reynolds number was 6000 based on the total discharge flow and the exit hole diameter. Tests were conducted at Reynolds numbers up to 30000, and no changes in flow character were observed.

Figures 4a and 4b are photographs of the flow in the axial midplane of the model with illuminated dye injection. The crank angle is 45 deg. after onset of discharge, for which the tips of the wraps are closely spaced and the discharge process has just begun. In Fig. 4a dye was injected in the left pocket and accelerates around the tip of the fixed scroll. (A pocket is the flow volume between an injector and the throat formed by the scroll tip and the adjacent wrap.) The dye in Fig. 4b was injected in the right pocket and accelerates around the tip of the orbiting scroll. The arrows sketched on the photographs indicate the flow patterns determined by observing the flow movement as recorded on video tape. It is apparent from Figs. 4a and 4b that at this crank angle the equal flows through each pocket enter the common discharge region and exit through the discharge port

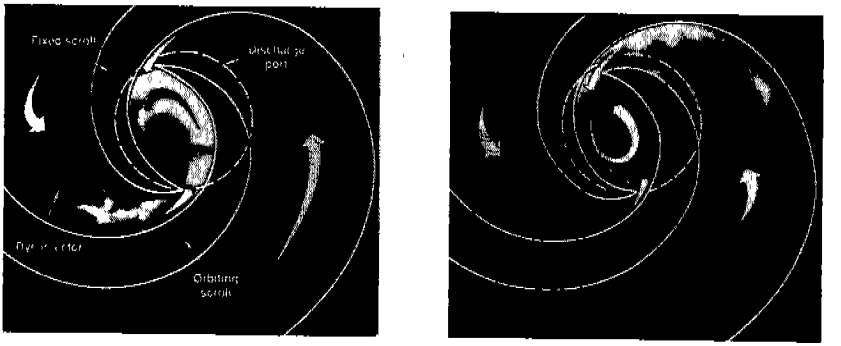

a) LEFT POCKET DYE INJECTION b) RIGHT POCKET DYE INJECTION

Fig. 4 Flow Visualization in Mid-Plane, $\theta_D = 45°$.

without entering the opposite pocket. The high velocity flows entering the central discharge region form a strong vortex in the region between the scroll tips. The flow leaving each throat region proceeds to drive the vortex in a counterclockwise direction. Note also the absence of dye in the eye of the vortex. Photographs of other laser illuminated planes show similar characteristics, indicating that the flow in the pocket is predominantly two-dimensional.

The photograph presented in Fig. 5 shows the flow in the axial midplane at a crank angle of 90

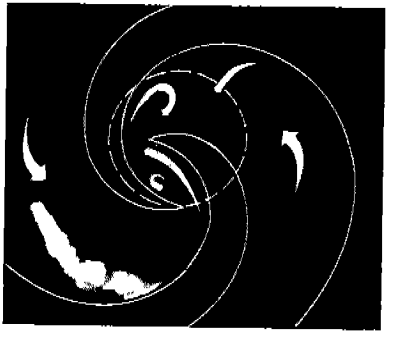

(DYE INJECTION FROM BOTH POCKETS)

Fig. 5 Flow Visualization in Mid-Plane, $\theta_D = 90°$.

deg. after onset of discharge with simultaneous dye injection in both pockets. At this crank angle the discharge hole is partially obstructed by the tip of the orbiting scroll. The flow is characterized by a separation region which exists near the tip of the fixed scroll. The flow from the left pocket is seen to pass between the scroll tips and penetrate into the right pocket, where a vortex forms. The opposing flow from the right pocket helps create this vortex and is consequently redirected. Note that this vortex is much weaker than at 45 deg. and is in the opposite direction. The dark area

located at the throat formed by the tip of the fixed scroll and the wrap of the orbiting scroll is the result of flow moving out of the plane of illumination.

Figure 6 is a photograph of the midplane flow at a crank angle of 180 deg. after onset of

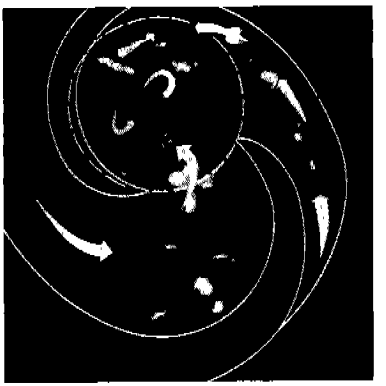

(DYE INJECTION FROM BOTH POCKETS)

Fig. 6 Flow Visualization in Mid-Plane, θ_D = 180°.

discharge. The discharge port is unobstructed at this crank angle. The flow from the left (bottom) pocket enters the discharge region and is surrounded by dyeless (dark) flow. This dark region is the result of flow from lower planes passing through the midplane. This flow from below the midplane exhibits a counter-rotating vortex structure. The flow from the right pocket appears to flow along the wrap of the fixed scroll. The in-plane patterns are much less distinct at this crank angle, and the vortex flows are weak in comparison to flows of other crank angles.

The effect of axial position was investigated by recording the flow characteristics for horizontal planes 11 percent and 89 percent of the height of the flow volume. The character of the flow in these planes was similar to what has been described for the midplane. However, the flow near the bottom surface (away from the discharge hole) was lower in velocity and less stable.

Air flow tests

To obtain quantitative data characterizing the pressure losses of the final compression and discharge region, air was used as the working fluid in the lucite model. Static pressure differences between the compression pockets and the discharge duct were measured as a function of crank angle and air flowrate.

The variation of loss coefficient, ξ, with crank angle for the right and left pockets is shown in Fig. 7. The difference in the loss coefficients of the two pockets is due to the asymmetries of the scroll geometry. The loss coefficient at 45 deg. is approximately five (5) times larger than the loss coefficient at 180 deg., indicating that the flow losses are largest at the onset of discharge. This result is not surprising, since this is also the point of maximum constriction of the flow area. Furthermore, the high velocities observed in the flow visualization tests at 45 deg. after onset of discharge corroborate that significant flow losses would exist. Results from similar tests conducted over a range of Reynolds numbers from 30000 to 76000 showed no variation of dimensionless loss coefficient with Reynolds number. The nondimensional loss coefficient, ξ, is defined as

$$\xi = \frac{P_{T1} - P_{T2}}{\frac{1}{2}\varrho V^2}$$

where

P_{T1} = total pressure in compression pocket (assumed equal to measured static pressure)

P_{T2} = total pressure in discharge duct (static pressure + $\frac{1}{2}\varrho V^2$)

ϱ = air density

V = mean flow velocity in discharge duct

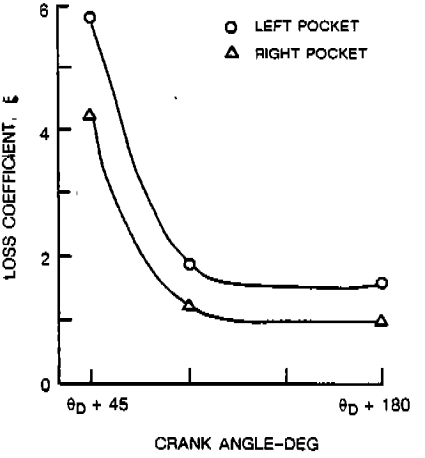

Fig. 7 Loss Coefficient vs. Crank Angle.

COMPUTATIONAL FLUID DYNAMICS STUDIES

Computational Fluid Dynamics (CFD) studies were conducted using the FIDAP CFD code (Ref. 2) to assist in understanding of the fluid flow characteristics in scroll compressors. FIDAP is a general purpose finite element computer program which solves the Navier–Stokes equations. The studies performed were companion to tests conducted in the Flow Visualization Facility as described previously. Three–dimensional computational flow models were developed to study the flow and its discharge from the central pocket region (innermost volume) at several crank angles that correspond to 45, 90, and 180 deg. after onset of discharge, (see Fig. 1). Since the tests were conducted with the scrolls positioned at a fixed crank angle, steady–state calculations were performed to give predictions of the detailed flow patterns. The calculations were made for water flow discharge conditions which simulate the experiment. Turbulent flow exists in the scroll configurations considered and was treated using a k–e turbulence model, (Ref. 2).

Crank angle of 45 deg. after onset of discharge

The calculated velocity field is shown in Fig. 8 for a crank angle of 45 deg. after onset of discharge. This crank angle as indicated in Fig. 1 represents a position where the scroll tips are in the early stage of separation. Fig. 8 shows three–dimensional velocity vectors at three individual planes which are at the top (discharge end), midplane, and near the bottom (outside the boundary layer). The flow volume is formed and bounded by two scroll wraps and by top and bottom walls. Discharge from the volume occurs only at the top plane and is via a circular port which envelops much of the region between the tips and extends slightly beyond the rightmost scroll tip (Fig. 8). The three–dimensional velocity vectors, depicted at the top plane, occur only within the bounds of the discharge port and are directed primarily upward.

The midplane velocity vectors characterize the general nature of the flow within the entire volume. The flow vectors indicate both the two–dimensional and the three–dimensional nature of the flow depending upon the location. The three–dimensional flow tends to move vertically upwards as it approaches the central section of the volume which is directly below the discharge port. The flow characteristic exhibited here possesses a strong axial component combined with an in–plane (horizontal) vortex flow component occurring at all axial levels. In contrast, within the rear regions of each half volume, the flow is essentially two dimensional, remaining in–plane with respect to axial injection position.

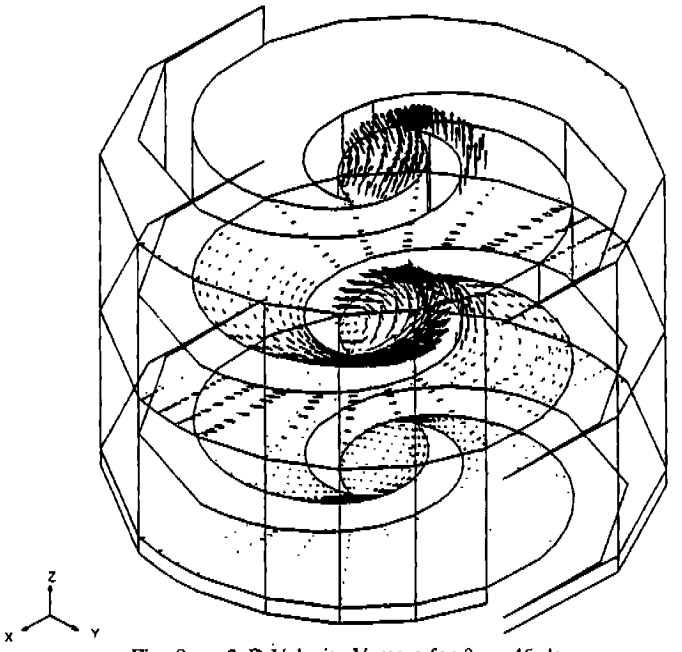

Fig. 8 3-D Velocity Vectors for θ_D + 45 deg.

A view of the flow in the axial midplane is shown in Fig. 9, where the velocity vectors are

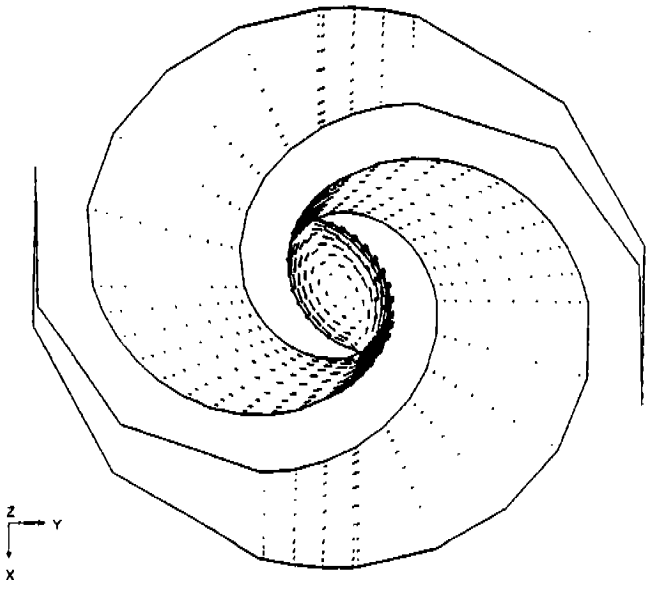

Fig. 9 Mid-Plane Velocity Vectors for θ_D + 45 deg.

projections of the actual three-dimensional vectors onto the midplane. The flow velocity vectors

indicate flow being injected in the rear of each half flow volume, being turned as it impinges on the opposing wall and proceeding towards the central region of the flow volume. In the central region, flow enters from both half flow volumes, passing through each throat region formed by the individual scroll tips and inner surface of the opposite scroll. A vortex flow develops in the central region. The calculated results show that this basic vortex flow pattern persists in this region throughout the entire axial extent of the flow volume. The velocity vectors shown in Fig. 9 can be compared to the photographs of the flow visualization experiments (see Figs. 4a and 4b), from which the flow has been categorized as having the same vortex pattern, again over the full axial extent of the volume. The calculations indicate that the flow passing through the discharge port is not uniform. This nonuniformity is exemplified in Fig. 10 in the form of a contour plot in which the height of the surface is proportional to the axial velocity component. Note that this component is essentially zero except within the region of the discharge port.

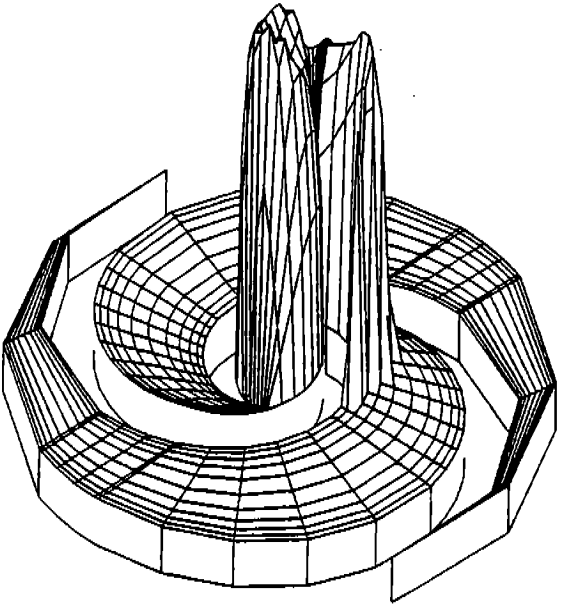

Fig. 10 Discharge Axial Velocity Component at θ_D + 45 deg.

Crank angle of 180 deg. after onset of discharge

As the discharge process continues in an actual scroll compressor, the moving scroll continues to move away from the fixed scroll. This action is associated with a progressively increased opening of the central region to the discharge port. This implies a less occluded and essentially unobstructed opening of the discharge port by the scroll tip regions for a crank angle of 180 deg. after onset of discharge. In addition, a less constrictive flow passage exists in the region of the scroll tips (see Fig. 1).

An interesting flow characteristic occurs at the discharge plane. In Fig. 11 an enlarged view of the discharge region shows the projection of the velocity vectors onto the discharge plane. A double vortex, albeit not strong (the in-plane velocity component several orders of magnitude less than axial velocity component), was predicted to form at the top of the flow volume. The double vortex flow pattern is being driven by the predominantly in-plane flow near the top of the volume, impinging upon the essentially upward moving flow originating from the lower region of the volume. The mass flux of the upward directed flow is highly peaked near that inside scroll surface

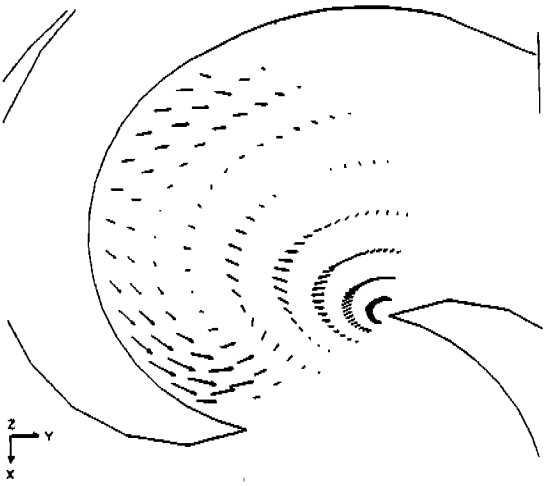

Fig. 11 Discharge Plane Velocity Vectors for θ_D + 180 deg.

which is located within the bounds of the discharge port region. The calculated results shown in Fig. 11 compare well with the flow visualization results presented in Fig. 6. Both the calculated velocity vectors and the photographs of the flow visualization tests show the occurrence of a double vortex flow characteristic at the top region of the flow volume.

Crank angle of 90 deg. after onset of discharge

At an intermediate crank angle (90 deg. after onset of discharge) similar type of flow calculations have been performed. Using the computed velocity flow field determined for this crank angle, particle trajectory calculations have been performed to illustrate the three-dimensional flow path of four samples of fluid as each travels from injection location to the discharge port. These results are shown in Fig. 12, where the representative fluid samples are located at the midplane. Two fluid samples are chosen from both the front injector and the rear injector. For the samples originating at the front injector, the trajectories are seen to proceed in an in-plane manner until reaching the vicinity of the flow volume which lies beneath the discharge port. At this point the fluid samples rise vertically until reaching the discharge port where the trajectory history is terminated. Note that the discharge port is located preferentially on the side of the front injector and that the fluid samples begin their upward movement and exit the volume upon initially coming under the influence of the discharge port.

For the two fluid samples originating at the rear or back injector, the fluid sample trajectories are seen to also follow an in-plane path until reaching the vicinity of the flow volume which lies beneath the discharge port. However, at this point the trajectory paths take a more circuitous route , first, moving past the first throat (formed by the first encountered scroll tip and inner surface of the opposite scroll), second, moving through the region bounded by the inner surfaces of each scroll tip. and, third, moving past the second throat (formed by the second encountered scroll tip and inner surface of the opposite scroll) before finally exiting the flow volume. In general, it appears that flow originally injected in the upper volume tends to exit when reaching the nearest edge of the discharge port, and that flow originally injected in the lower volume tends to be pushed towards the central region of the discharge port. Fluid sample trajectories at the other crank angles show similar results.

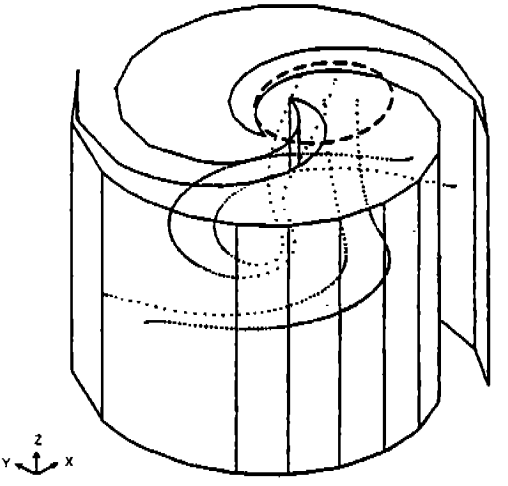

Fig. 12 3-D Particle Trajectories for θ_D + 90 deg.

SUMMARY

A Flow Visualization Facility was developed to provide a means of studying the flow loss mechanisms in scroll compressor geometries. Dye injection was demonstrated as a diagnostic technique to visually identify regions of localized vortex flow. This technique was used to extensively map the complete flow volume. Flow visualization tests were conducted over a range of Reynolds numbers between 6000 and 30000. The results of these experiments showed no significant differences in general flow structure for specific crank angle configurations as the Reynolds number (flowrate) was varied. Also, the Facility was used to determine the pressure loss coefficient as a function of crank angle. The pressure loss coefficient is approximately five (5) times greater at a crank angle 45 deg. after onset of discharge in comparison to the loss coefficient at a crank angle 180 deg. after onset of discharge.

A three dimensional computational model was developed to provide insight into the flow visualization experiment and to aid in both understanding the results and setting the direction of future experimental configurations. A comparison between the experimental and the calculated results shows good agreement. Flow characteristics reflecting complex vortex flow patterns were predicted and were corroborated by the experimental results.

REFERENCES

1. Hirano, T., et al.,: Development of High Efficiency Scroll Compressors for Heat Pump Air Conditioners, Mitsubishi Heavy Industries, Ltd., Tech. Rev. Vol. 26, No. 3, Oct. 1989.

2. Engelman, M. S.: FIDAP- A Fluid Dynamics Analysis Package, Adv. Eng. Soft. Vol. 4, No. 4, pp.163-166, 1982.